

Stromal cues regulate the pancreatic cancer epigenome and metabolome

Mara H. Sherman^{a,1}, Ruth T. Yu^a, Tiffany W. Tseng^a, Cristovao M. Sousa^b, Sihao Liu^a, Morgan L. Truitt^a, Nanhai He^a, Ning Ding^a, Christopher Liddle^c, Annette R. Atkins^a, Mathias Leblanc^a, Eric A. Collisson^d, John M. Asara^e, Alec C. Kimmelman^{b,f}, Michael Downes^{a,2}, and Ronald M. Evans^{a,g,2}

^aGene Expression Laboratory, Salk Institute for Biological Studies, La Jolla, CA 92037; ^bDivision of Genomic Stability and DNA Repair, Department of Radiation Oncology, Dana-Farber Cancer Institute, Harvard Medical School, Boston, MA 02215; ^cStorr Liver Centre, Westmead Millennium Institute, Sydney Medical School, University of Sydney, Sydney, NSW 2006, Australia; ^dDepartment of Medicine/Hematology and Oncology, University of California, San Francisco, CA 94143; ^eDivision of Signal Transduction, Department of Medicine, Beth Israel Deaconess Medical Center, Boston, MA 02115; ^fDepartment of Radiation Oncology, New York University School of Medicine, New York, NY 10016; and ^gHoward Hughes Medical Institute, Salk Institute for Biological Studies, La Jolla, CA 92037

Contributed by Ronald M. Evans, December 14, 2016 (sent for review October 18, 2016; reviewed by Scott M. Lippman and Richard Posner)

A fibroinflammatory stromal reaction cooperates with oncogenic signaling to influence pancreatic ductal adenocarcinoma (PDAC) initiation, progression, and therapeutic outcome, yet the mechanistic underpinning of this crosstalk remains poorly understood. Here we show that stromal cues elicit an adaptive response in the cancer cell including the rapid mobilization of a transcriptional network implicated in accelerated growth, along with anabolic changes of an altered metabolome. The close overlap of stroma-induced changes in vitro with those previously shown to be regulated by oncogenic Kras in vivo suggests that oncogenic Kras signaling—a hallmark and key driver of PDAC—is contingent on stromal inputs. Mechanistically, stroma-activated cancer cells show widespread increases in histone acetylation at transcriptionally enhanced genes, implicating the PDAC epigenome as a presumptive point of convergence between these pathways and a potential therapeutic target. Notably, inhibition of the bromodomain and extraterminal (BET) family of epigenetic readers, and of Bromodomain-containing protein 2 (BRD2) in particular, blocks stroma-inducible transcriptional regulation in vitro and tumor progression in vivo. Our work suggests the existence of a molecular “AND-gate” such that tumor activation is the consequence of mutant Kras and stromal cues, providing insight into the role of the tumor microenvironment in the origin and treatment of Ras-driven tumors.

pancreatic ductal adenocarcinoma | tumor microenvironment | cancer metabolism | BRD2 | histone acetylation

The tissue microenvironment plays important roles in directing development and differentiation but is also required for normal tissue homeostasis, working in part through secreted factors that control epithelial cell growth and survival (1). Disruptions in this tissue homeostatic mechanism accompany solid tumor progression, enabling cancer cells to overcome the barriers to tumorigenesis imposed by normal tissue architecture (2). In pancreatic ductal adenocarcinoma (PDAC), the dense fibroinflammatory stroma is largely attributed to soluble and extracellular matrix components secreted by cancer-associated fibroblasts [CAFs; derived predominantly from activated pancreatic stellate cells (PSCs)] (3).

The microenvironment surrounding PDAC undergoes dynamic alterations including aberrant immune responses and the accumulation of a fibroinflammatory stroma (4, 5), alterations co-opted from the wound-healing response (6). This cellular compartment not only cooperates with oncogenic alterations to drive pancreatic tumorigenesis (7, 8) but compromises the efficacies of cytotoxic and immune-targeted therapies (9–12). Stromal alterations during pancreatic tumorigenesis include activation of tissue-resident stellate cells: Although stellate cells contribute to tissue homeostasis and maintenance of the basement membrane under normal conditions (13), these cells transdifferentiate into myofibroblast-like cells in the context of tissue damage or during pancreatic tumor progression (14). PSC activation features robust induction of a transcriptional program that drives a fibroinflammatory response, including

extracellular matrix components, cytokines, and growth factors (15). Activated PSCs are a rich repository for secreted factors that may have diverse effects on neighboring epithelial cells, yet the nature of this interaction remains incompletely understood. Indeed, recent work suggests both tumor-supportive (16, 17) and tumor-suppressive or homeostatic (18–20) roles for the PDAC-associated stroma, suggesting that an improved understanding of the molecular basis of tumor–stroma interactions may enable identification and targeting of tumor-supportive mechanisms.

Results

To explore the role of CAF-derived signals in gene regulation in the PDAC epithelial compartment, pancreatic cancer cells were

Significance

Stromal fibroblasts of the pancreatic tumor microenvironment (TME) have been shown to play both tumor-supportive and tumor-suppressive roles in enacting a dysregulated wound-healing response. This apparent complexity suggests that an improved understanding of the molecular basis of cell–cell interactions in the TME is required to identify and target stroma-derived, growth-permissive mechanisms. Here we show that stromal cues induce transcriptional and metabolic changes in pancreatic cancer cells implicated in anabolic metabolism, which overlap with those previously demonstrated downstream of oncogenic Kras. Stromal signals broadly induce histone acetylation in the pancreatic cancer epigenome, and we highlight inhibition of acetyl-lysine sensing by the bromodomain and extraterminal (BET) bromodomain family, Bromodomain-containing protein 2 (BRD2) in particular, as a potential therapeutic strategy.

Author contributions: M.H.S., C.M.S., E.A.C., A.C.K., M.D., and R.M.E. designed research; M.H.S., T.W.T., C.M.S., S.L., M.L.T., N.H., E.A.C., and J.M.A. performed research; M.H.S., R.T.Y., C.M.S., C.L., M.L., E.A.C., A.C.K., M.D., and R.M.E. analyzed data; and M.H.S., R.T.Y., N.D., A.R.A., M.D., and R.M.E. wrote the paper.

Reviewers: S.M.L., UC San Diego Moores Cancer Center; and R.P., Northern Arizona University.

Conflict of interest statement: M.H.S., R.T.Y., N.D., A.R.A., M.D., and R.M.E. are coinventors of technologies using BET inhibitors and may be entitled to royalties. A.C.K. is an inventor on patents pertaining to Kras regulated metabolic pathways; redox control pathways in pancreatic cancer, targeting GOT1 as a therapeutic approach; and the autophagic control of iron metabolism. A.C.K. is on the Scientific Advisory Board of Cornerstone Pharmaceuticals and is a founder of Vescor Therapeutics.

Freely available online through the PNAS open access option.

Data deposition: RNA-Seq data can be accessed in the NCBI Sequence Read Archive (accession nos. [SRP059641](#) and [SRP059642](#)), and ChIP-Seq data have been deposited in Gene Expression Omnibus (GEO) (accession no. [GSE70971](#)).

¹Present address: Department of Cell, Developmental & Cancer Biology, Oregon Health & Science University, Portland, OR 97201.

²To whom correspondence may be addressed. Email: evans@salk.edu or downes@salk.edu.

This article contains supporting information online at www.pnas.org/lookup/suppl/doi:10.1073/pnas.1620164114/-DCSupplemental.

grown in hyaluronic acid-based hydrogels in the presence (stromal) or absence (astromal) of collagens and soluble stromal cues (from patient-derived CAFs or in vitro activated PSCs, which secrete similar levels of cytokines, growth factors, ECM components, and remodeling factors) (15). In response to stromal cues, PDAC cell lines grown in this 3D culture system increased the expression of the secreted factors *CSF2* and *CXCL1*, without any apparent change in morphology or initial cell growth (Fig. 1A and B and Fig. S1A). Furthermore, RNA-seq analyses showed broad effects of stromal inputs on transcription, with the expression of 332 and 128 genes up- and down-regulated, respectively, in MIAPaCa2 cells and 480 up-regulated and 406 down-regulated genes in p53 2.1.1 cells (>1.5-fold; Fig. 1C). KEGG enrichment analyses of significantly up-regulated genes identified similar pathways activated in p53 2.1.1 and MIAPaCa2 cells, including cell cycle, DNA replication, and metabolic pathways (Fig. 1D and

Fig. S1B). Indeed, a stroma-inducible signature, defined as the 86 genes up-regulated by stromal cues in both MIAPaCa2 and p53 2.1.1 cell lines, is enriched for genes in metabolic pathways as well as nucleoporins (Fig. 1E), pathways shown to be up-regulated during pancreatic cancer progression in mice (21). The induction of selected genes was validated by quantitative PCR (qPCR) (Fig. 1F and Fig. S1C). Importantly, similar effects of stromal cues are evident in laser-microdissected human pancreatic cancer (Fig. 1G; low *IL6* expression indicates little stromal contamination of tumor samples). Collectively, these results indicate that the stromal secretome is sufficient to regulate the expression of diverse gene classes in pancreatic cancer cells.

Interestingly, the gene sets induced by stromal cues in vitro overlap significantly with those activated by an inducible allele of *Kras*^{G12D} in vivo (22), suggesting that permissive signals from stroma drive oncogene-driven transcription in vivo (Fig. 2A). This finding is consistent with reports that a fibroinflammatory stromal reaction cooperates with oncogenic alterations in *Kras* to drive pancreatic cancer progression, whereas mutant *Kras* alone is insufficient to drive tumorigenesis (8). Supporting this apparent functional convergence, qPCR analyses confirm that the stromal secretome up-regulates genes across multiple functional categories, including downstream *Kras*^{G12D} targets involved in immune modulation (e.g., *Csf2*) (23, 24) and anabolic metabolism (e.g., *Rrm2*, *Sc4mol*) (Fig. 2B). Consistent with changes in metabolic genes, stroma-activated PDAC cells consumed more glucose (~40–90%; Fig. 2C and Fig. S2A and B) and secreted more lactate (40–60%; Fig. 2D), without significant effects on glutamine consumption (Fig. S2C). Furthermore, intracellular metabolomics revealed that stromal cues dramatically alter cellular metabolism, increasing intermediates in glycolysis, the pentose phosphate pathway, downstream steps in nucleic acid synthesis, and the TCA cycle (Fig. 2E and Fig. S2D). Although PDAC cells grow to a similar extent in the presence or absence of stromal cues under nutrient-replete conditions (Fig. S1A), human pancreatic tumors are nutrient-poor and in particular feature low levels of glucose and glutamine (25). Under nutrient-deprived conditions relevant to the microenvironment of human PDAC, stromal cues significantly increased the viability of PDAC cells, consistent with paracrine activation of an adaptive transcriptional survival program (Fig. 2F). Together, these results suggest that the stromal reaction marshals genomic and metabolic responses in PDAC cells that enforce oncogenic signaling.

To understand how the stroma authorizes gene expression in PDAC cells, we explored acute changes in histone acetylation marks that differ between stroma-rich and stroma-poor regions of human PDAC (26), although we do not exclude effects of additional histone marks. Accordingly, PDAC cells exposed to soluble stromal cues showed increased levels of acetylation at both H3K9 (a marker of active promoters) and H3K27 (a marker of active enhancers; Fig. 3A). Oncogenic *Kras* induces histone acetylation in vivo (27), implicating epigenetic alterations as a putative point of convergence between oncogenic and microenvironmental signals. A time course revealed surprisingly rapid changes in histone acetylation, detectable within 1–3 h (Fig. 3B), arguing against a requirement for de novo protein synthesis to induce these acetylation changes. To understand the transcriptional consequences of these epigenetic alterations, we localized sites of differential histone acetylation using targeted (ChIP-qPCR) and global (ChIP-Seq) analyses in PDAC cells grown under astromal or stromal conditions. Notably, stromal cues dramatically increased H3K9 acetylation in promoter regions across the genome (Fig. 3C and D). The top 5% of differentially acetylated protein-coding genes are enriched for cancer pathways, including pancreatic cancer (Fig. 3E), suggesting that stromal cues achieve their impact in part by coordinated chromatin-dependent remodeling of functionally related gene sets. Consistent with these genome-wide studies, site-specific ChIP-qPCR revealed increased

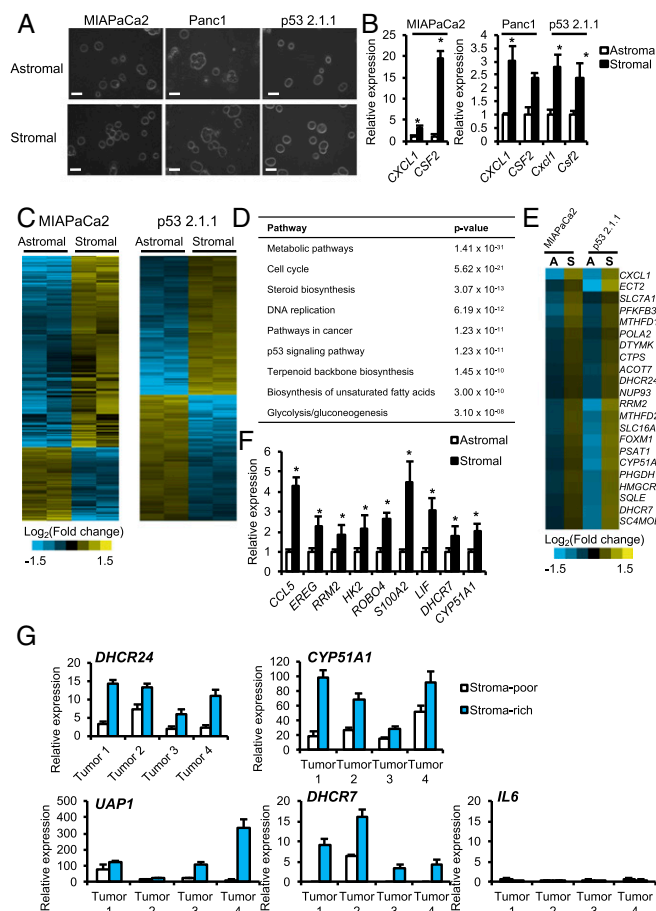


Fig. 1. Stromal cues drive distinct gene expression patterns in PDAC cells. (A) Brightfield images of PDAC cells in astromal or stromal cultures after 48 h. (Scale bar, 50 μ m.) (B) Gene expression after 48 h in astromal or stromal cultures, measured by qPCR and normalized to *36B4* ($n = 3$). (C) Heat maps representing gene expression, measured by RNA-Seq and representing normalized and \log_2 -transformed FPKM. Genes changed at least 1.5-fold are shown. (D) Results of KEGG enrichment analysis of genes significantly up-regulated by stromal cues ($P < 0.05$) in p53 2.1.1 cells. (E) Heat map representing a selected subset of stroma-inducible signature genes, significantly up-regulated by stroma cues in both of the indicated cell lines. (F) Gene expression in MIAPaCa2 cells after 48 h in astromal or stromal cultures, measured by qPCR and normalized to *36B4* ($n = 3$). (G) Gene expression in human PDAC samples from stroma-poor or stroma-rich regions, isolated by laser capture microdissection, $n = 4$ with 3–10 regions of each type isolated per tumor sample. Values were normalized to *GAPDH*. Data are presented as the mean \pm SD; * $P < 0.05$ by unpaired two-tailed Student's t test.

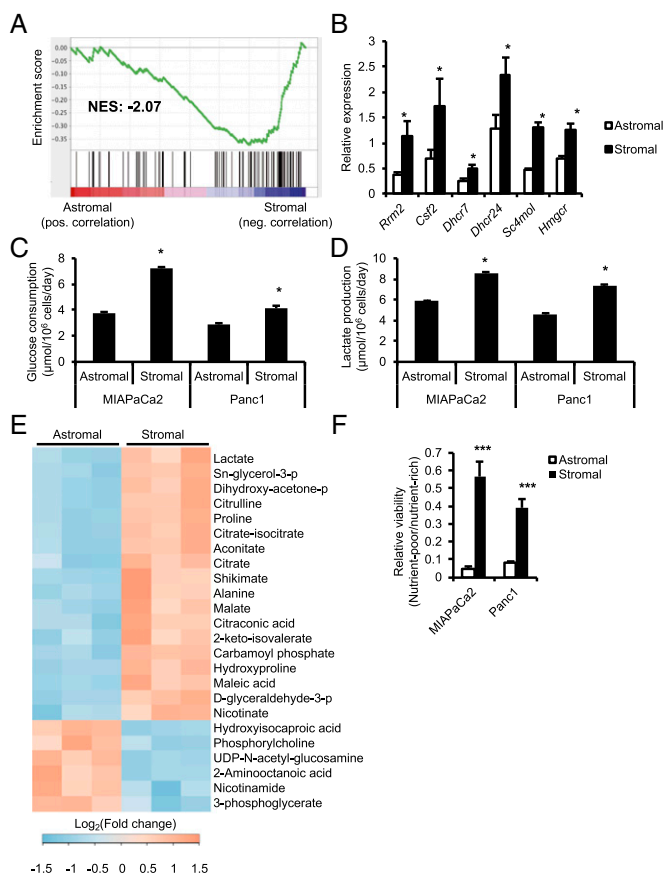


Fig. 2. Stroma-inducible alterations in gene expression and metabolism are functionally complementary to oncogenic Kras. (A) GSEA enrichment plot comparing genes up-regulated by stromal cues (in p53 2.1.1 cells, to compare mouse vs. mouse gene sets) and genes down-regulated upon Kras extinction as determined by Ying et al. (22). Normalized enrichment score (NES) is reported. (B) Gene expression of previously reported Kras-regulated genes in p53 2.1.1 cells after 48 h in astromal or stromal cultures, measured by qPCR and normalized to 36B4 ($n = 3$). (C and D) MIAPaCa2 and Panc1 cells were grown for 48 h in astromal or stromal conditions, then switched to fresh DMEM containing 2% (vol/vol) FBS. Media samples were collected after 24 h and compared with fresh media. (C) Glucose consumption and (D) lactate production by the indicated cell lines. (E) Heat map representing intracellular metabolites significantly regulated by stromal cues in MIAPaCa2 cells as determined by targeted liquid chromatography–MS/MS using SRM. MIAPaCa2 cells were cultured under astromal or stromal conditions for 48 h, at which point metabolite levels were measured from triplicates for each condition. (F) Viability of MIAPaCa2 and Panc1 cells grown in astromal or stromal conditions in the presence of high glucose and glutamine, or reduced glucose and glutamine, for 48 h (see *SI Materials and Methods* for details). * $P < 0.05$, *** $P < 0.0005$ by unpaired two-tailed Student's t test.

acetylation at promoter and enhancer regions in the context of stromal signals (Fig. 3F). These results demonstrate that microenvironmental cues rapidly regulate histone acetylation at a subset of promoters and enhancers in PDAC cells.

Given the extent of the epigenetic changes, we postulated that effectors of this paracrine regulation may be susceptible to therapeutic inhibition. To explore this notion, we targeted the interaction between acetylated histone tails and chromatin readers. As acetylated histone marks are known targets of bromodomain and extraterminal (BET) bromodomain-containing proteins (28–31), we explored the impact of the BET bromodomain inhibitor JQ1 on stroma-inducible gene expression in vitro and on tumor growth in vivo. Interestingly, although treatment of pancreatic tumor cells with JQ1 reduced the expression of hundreds of

genes under both astromal and stromal conditions, about 450–475 genes were uniquely down-regulated by JQ1 under stromal conditions (Fig. S3A). Notably, in the PDAC cell lines examined, this subset of genes (Fig. 4A and B and Fig. S3B) significantly overlaps (35–60%) with those induced by stromal cues, suggesting inverse transcriptional regulation by microenvironmental signals and JQ1. By extension, viability in the context of stromal cues was significantly reduced by JQ1 treatment in multiple PDAC cell lines, albeit to varying degrees (Fig. S3C). Antitumor activity of JQ1 in pancreatic cancer has been described previously by Mazur et al. (32); in this study, the authors suggest that the antitumor effects of BET inhibition are likely due to effects on MYC as well as negative regulation of inflammatory gene expression. In agreement with this work, we observed down-regulation of Myc with JQ1 treatment in the p53 2.1.1 line by

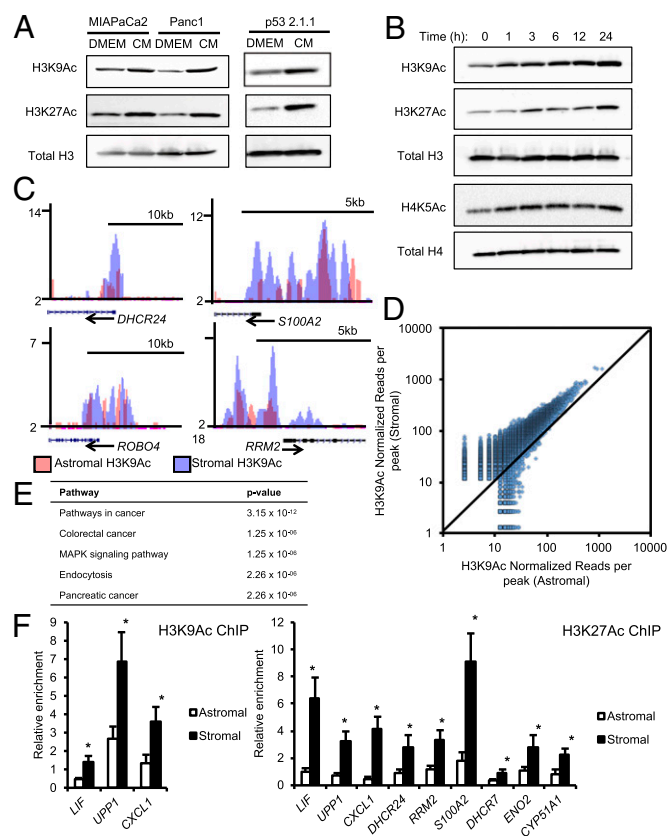


Fig. 3. Histone acetylation at a subset of promoters and enhancers in PDAC cells is regulated by microenvironmental signals. (A) Western blots for histone modifications or total histone H3 using acid-extracted histones from the indicated cell lines, after 24 h in the presence of DMEM or patient-derived stromal fibroblast CM (Left) or primary activated mouse PSC CM (Right) (preparation described in *SI Materials and Methods*). (B) Western blot for histone modifications or total histone H3 using acid-extracted histones from MIAPaCa2 cells after exposure to stromal fibroblast CM for the indicated time. (C) University of California, Santa Cruz (UCSC) genome browser tracks from ChIP-Seq data for H3K9Ac in MIAPaCa2 cells under astromal (pink) and stromal (blue) conditions. (D) Scatter plot demonstrating global normalized reads per peak from H3K9Ac ChIP-Seq under astromal (x axis) versus stromal (y axis) conditions. The black line is $x = y$. (E) Results of KEGG enrichment analysis of the top 5% of differentially acetylated (stromal > astromal) protein-coding genes as determined by H3K9Ac ChIP-Seq. (F) ChIP for H3K9Ac (Left) and H3K27Ac (Right) in MIAPaCa2 cells followed by qPCR for promoter and enhancer regions of the indicated genes identified in the ChIP-Seq datasets. Values were normalized to a negative control region for each condition. Data are presented as the mean + S.D. of triplicate experiments. * $P < 0.05$, determined by unpaired two-tailed Student's t test.

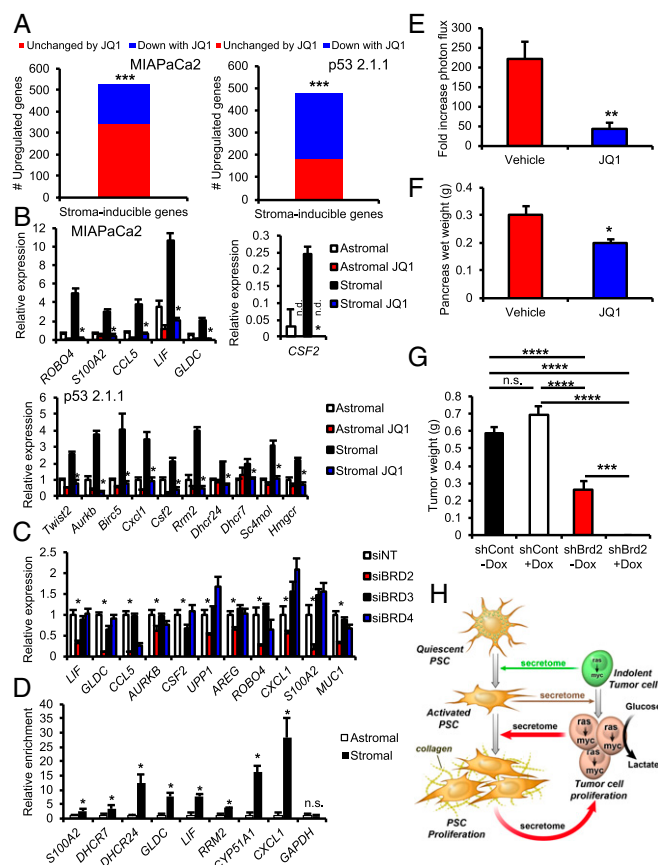


Fig. 4. BET bromodomains are transducers of stroma-inducible epigenetic changes, and BET inhibition reduces PDAC growth in vivo. (A) Proportion of stroma-inducible genes significantly down-regulated by JQ1 under stromal conditions in the indicated cell lines. *** $P < 0.0001$ by Fisher's exact test, comparing all genes down-regulated by JQ1 under stromal conditions and all genes up-regulated under stromal (vs. astromal) conditions in each cell line. (B) Gene expression after 48 h in astromal or stromal cultures \pm treatment with 500 nM JQ1 for the final 16 h of the experiment, measured by qPCR and normalized to *36B4*. Data are presented as the mean \pm SD of triplicate wells from a representative experiment. * $P < 0.05$ by unpaired two-tailed Student's *t* test (comparing Stromal and Stromal JQ1). n.d., not detected. (C) Gene expression in MIAPaCa2 cells expressing the indicated siRNA (NT, nontargeting) after 48 h in stromal conditions, measured by qPCR and normalized to *36B4*. Analysis was performed 72 h posttransfection. Data are presented as the mean \pm SD of triplicate wells from a representative experiment. * $P < 0.05$ by unpaired two-tailed Student's *t* test (comparing siNT and siBRD2). (D) ChIP-qPCR for BRD2 in MIAPaCa2 cells under astromal or stromal conditions, using promoter regions identified by ChIP-Seq. Data are normalized to an intergenic region and presented as the mean \pm SD of triplicate experiments. * $P < 0.05$ by unpaired two-tailed Student's *t* test. (E) Fold change in photon flux (photons per second) in pancreatic tumors after 14 d of treatment with vehicle [10% hydroxypropyl- β -cyclodextrin in water (vol/vol), $n = 9$] or JQ1 (75 mg/kg JQ1, $n = 8$). ** $P < 0.005$ by unpaired two-tailed Student's *t* test. (F) Pancreas wet weights at experimental endpoint from mice treated as described in E. * $P < 0.05$ by unpaired two-tailed Student's *t* test. (G) Tumor weights at experimental endpoint (18 d on or off doxycycline; 29 d posttransplantation). shControl (shCont) -Dox: $n = 5$; shControl +Dox: $n = 8$; shBrd2 -Dox: $n = 8$; shBrd2 +Dox: $n = 8$. P values determined by one-way ANOVA and Bonferroni post hoc test; *** $P < 0.001$; **** $P < 0.0001$; n.s., not significant. (H) Model depicting the complex interplay between stromal fibroblast-derived signals and pancreatic cancer cells in the TME.

RNA-seq but not in the MIAPaCa2 line. However, a number of inflammatory genes were down-regulated by JQ1 in both cell lines, consistent with the findings of Mazur et al., including *IFIT2*, *IFIT3*, *IRF5*, *CXCL5*, and *CXCL2* in MIAPaCa2 cells and

IL34, *C3*, *Cxcl1*, *Ccl2*, and *Cxcl5* in p53 2.1.1 cells. The expression of BET family members Bromodomain-containing proteins 2, 3, and 4 (BRD2, BRD3, and BRD4) (33, 34) in PDAC lines (Fig. S3D) raises the question as to which might be dominant in stroma-activated gene expression. Unexpectedly, BRD2 knock-down most closely phenocopied JQ1 treatment and down-regulated genes induced under stromal conditions (Fig. 4C). This is confirmed by increased BRD2 binding to promoters of stroma-inducible genes, measured by ChIP assay (Fig. 4D). These findings make an interesting contrast with the recent observation that stellate cell activation during the stromal response is principally mediated by BRD4 (35), suggesting the potential for cell-specific functions of different BET bromodomain proteins in the tumor ecosystem.

To assess whether disruption of BET family activity could affect pancreatic tumor growth in vivo, we used orthotopic transplantation of luciferase-labeled PDAC cells into the pancreata of syngeneic hosts (Fig. S4A). Impressively, JQ1 treatment significantly reduced pancreatic tumor growth and pancreas wet weight at the study endpoint (Fig. 4E and F and Fig. S4B), consistent with previous results (32, 36). In addition, significant reductions in proliferation and immune cell infiltration were seen (Fig. S4C and D), consistent with the negative regulation of transcriptional programs promoting anabolic metabolism and inflammation. To assess the specific role of BRD2, we transduced luciferase-labeled p53 2.1.1 PDAC cells with a doxycycline-inducible shRNA targeting *Brd2* (Fig. S5A and B) before orthotopic transplantation (Fig. S5C and D). Notably, doxycycline treatment significantly reduced pancreatic tumor growth by over 50%, correlating with the reduced BRD2 protein levels in the tumors (Fig. S5E–G). When this study was performed alongside a doxycycline-inducible nontargeting control hairpin and an independent inducible shBrd2 clone, tumor growth in the control group was unaffected by doxycycline, whereas tumor growth in the inducible shBrd2 group was significantly reduced by doxycycline (Fig. S5H). To confirm these results in a different system, FC1245 PDAC cells derived from KPC mice were transduced with inducible shBrd2 or an inducible control hairpin as described above and used for orthotopic transplantation. Doxycycline significantly reduced tumor growth in the inducible shBrd2 line, whereas the control cell line was unaffected by doxycycline treatment (Fig. 4G). Significant growth differences were noted between the shControl and shBrd2 cell in vivo in the absence of doxycycline, which may reflect leaky expression of shBrd2 in vivo in this system or may indicate a less aggressive clone. These results directly implicate the BET family of proteins as a viable therapeutic target in pancreatic cancer, in part due to effects on gene expression via transduction of the cancer epigenome.

Discussion

Despite the well-acknowledged role of the TME in modulating tumor growth and progression, an underlying molecular mechanism illuminating its effect is rudimentary at best. We show that a cell-free extract of secreted factors from cultured stromal cells is sufficient to dramatically alter survival of cultured PDAC cell lines under relevant conditions of nutrient challenge. This survival response is linked to a rapid change in transcriptional networks driving core metabolic pathways in the TCA cycle, anabolic metabolism and cell growth. The demonstration that the micro-environmental context broadly influences the epigenetic state of the tumor suggests that either side of this dynamic equation—tumor or tumor microenvironment (TME)—can individually or possibly cooperatively serve as therapeutic targets. Interestingly, recent work has shown that tissue-specific microenvironmental signals can shape chromatin landscapes to support cellular function in distinct populations of resident macrophages (37, 38). Together with our work, these studies raise the possibility that micro-environmental context broadly influences the epigenetic state of

tissue-resident cell types under physiological and pathological conditions. In the context of the wound-like TME, TME-induced transcriptional and metabolic changes overlap with those induced by oncogenic Kras, which presumably on its own cannot fully enable proliferation and viability in a nutrient-poor microenvironment. Although we have not identified a specific microenvironment-derived factor that regulates transcription and metabolism in a paracrine manner, our previous work identified numerous secreted factors that are transcriptionally up-regulated during stromal activation in pancreatic cancer and that may serve to regulate transcription and metabolism in the epithelial compartment (15). These include factors that activate Ras-MAPK signaling via cell surface receptors to augment MYC activity, including connective tissue growth factor (39), hepatocyte growth factor (40), and insulin-like growth factor binding proteins 2, 3, and 7 (which signal to EGFR indirectly via sphingosine-1-phosphate) (41). Stromal PSCs also produce Il6, which can activate STAT3 in a paracrine manner to transcriptionally activate MYC (42–44) and induce associated metabolic and transcriptional changes. We propose that microenvironmental regulation of gene expression cooperates with cell-autonomous pathways to fortify cancer cell viability by co-opting an otherwise normal, and usually transient, wound-healing response. Collectively, this work describes a connection between the stromal response and a driver oncogene (Fig. 4H) and may offer new insights into the role of the microenvironment and the treatment of Ras-driven tumors.

Materials and Methods

Cell Culture. Cell lines MIA PaCa2, Panc1, and AsPC1 were obtained from the American Type Culture Collection. The p53 2.1.1 cell line was provided by Eric Collisson, University of California, San Francisco (45) and was derived from PDAC from a FVB/n Kras^{LSL-G12D/+}; Trp53^{flox/+}; Ptf1a-Cre mouse. The FC1245 cell line was provided by David Tuveson, Cold Spring Harbor Laboratory, Cold Spring Harbor, NY, and was derived from a C57BL/6J Kras^{LSL-G12D/+}; Trp53^{LSL-R172H/+}; Pdx1-Cre mouse. Mouse PSCs were isolated from healthy pancreata of wild-type C57BL/6J mice aged 6–12 wk by density centrifugation, as previously described (15). Human cancer-associated stromal myofibroblasts were grown out of surgically resected PDAC samples as described previously (33) and provided by J. A. Drebin and P. J. O'Dwyer, University of Pennsylvania, in accordance with the Institutional Review Boards of the Salk Institute and the University of Pennsylvania. The stromal population was confirmed to lack KRAS exon 2 mutations and was immortalized with SV40 large T antigen (pLenti-SV40-T, Applied Biological Materials Inc.) at a MOI of 2. This immortalized cell line was used for consistent generation of conditioned media for stromal cultures (described in *3D Astromal and Stromal Culture Generation* below.). DMEM and RPMI 1640 were purchased from Life Technologies, and characterized FBS was purchased from HyClone. DMEM containing 10% (vol/vol) FBS was used to culture MIA PaCa2, Panc1, p53 2.1.1, and FC1245 cell lines as well as mouse PSCs and human PDAC-associated stromal myofibroblasts. RPMI 1640 containing 10% (vol/vol) FBS was used to culture AsPC1 cells.

3D Astromal and Stromal Culture Generation. Astromal and stromal cultures were generated using the ESI BIO HyStem-C kit (BioTime, Inc.). Kit components were equilibrated to room temperature, and the suggested volume of degassed H₂O was transferred to vials of Extralink (PEGDA), Gelin-S (thiol-modified denatured collagen), and Glycosil (thiol-modified hyaluronan) using a syringe and 25G needle to avoid opening the vials. Vials were vortexed every 5–10 min to aid reconstitution, and all reagents were in solution within 30 min. To generate astromal cultures, PDAC cells were resuspended in a solution of 1:1:1 degassed H₂O:Glycosil:Extralink at a concentration of 5 × 10⁵ cells per mL. After careful mixing by pipetting, the suspension was added to a culture dish and placed in a 37 °C incubator for 30 min to polymerize. To generate stromal cultures, PDAC cells were resuspended in a solution of 1:1:1 Gelin-S (collagens):Glycosil:Extralink at a concentration of 5 × 10⁵ cells per mL, mixed by pipetting, and added to a culture dish. After 30 min in a 37 °C incubator, both astromal and stromal cultures polymerized and the appropriate volume of DMEM containing 10% (vol/vol) FBS was layered over the hydrogels. The next day, media was removed, gels washed twice with sterile PBS, and DMEM containing 2% (vol/vol) FBS was added to astromal cultures or conditioned media containing 2% (vol/vol) FBS was added to stromal cultures. Cells appeared in single-cell suspension upon

plating and expanded as spheroids over several days in 3D culture. Conditioned media for human PDAC lines was generated from immortalized stromal myofibroblasts grown out of surgically resected human PDAC. Stromal cells were grown to confluency and changed to fresh DMEM containing 2% (vol/vol) FBS. After 48 h, media was collected, spun down at 300 × g for 5 min to remove dead cells and debris, and added to stromal cultures. Conditioned media for murine PDAC lines was generated from activated mouse PSCs. PSCs were isolated from wild-type C57BL/6J mice 6–12 wk of age; yield from five mice was pooled into one T25 flask and cultured for 7 d in DMEM containing 10% (vol/vol) FBS to generate confluent activated PSCs or myofibroblast-like cells. On day 7, media was changed to fresh DMEM containing 2% (vol/vol) FBS, and after 48 h, media was collected, spun down at 300 × g for 5 min to remove dead cells and debris, and added to stromal cultures. For applications requiring recovery of a single-cell suspension (i.e., ChIP or cell counting for metabolic assays), hydrogels were constructed as described above but using PEGSSDA (sold separately by BioTime, Inc.) as a cross-linker for both astromal and stromal conditions. Volumetric ratios were as listed above, but the PEGSSDA reagent was reconstituted at a 2× concentration to ensure efficient polymerization of the hydrogels.

Gene Expression Analysis from 3D Cultures. For RNA isolation from 3D cultures, TRIzol (Life Technologies) was added to each well (the same volume as the hydrogel volume per well). TRIzol and hydrogel were resuspended by pipetting up and down through a cut pipet tip, transferred to 2.8-mm ceramic bead tubes, and homogenized at 3,000 rpm for 20 s in a PowerLyzer 24 (tubes and homogenizer; MO BIO Laboratories, Inc.). RNA isolation was then performed per the manufacturer's protocol. Reverse transcription was performed using the iScript cDNA Synthesis Kit per the manufacturer's protocol (Bio-Rad Laboratories, Inc.), and qPCR was carried out using SYBR Green master mix on a CFX384 Real-Time PCR Detection System (Bio-Rad Laboratories, Inc.). Primer sequences are provided in [Dataset S1](#).

RNA-Seq. RNA-Seq from astromal and stromal conditions was performed after 24 h of conditioned media addition or 48 h of growth in 3D culture. JQ1 treatments (500 nM, provided by J. Bradner, Dana-Farber/Harvard Cancer Center) were administered for the last 16 h of culture. Total RNA was isolated using TRIzol (Life Technologies) and the RNeasy mini kit with on-column Dnase digestion (QIAGEN). Library preparation, sequencing, and analysis procedures are described in [SI Materials and Methods](#).

Metabolite Measurements. Glucose, lactate, and glutamine consumption were measured using a YSI 2950 analyzer. For this, PDAC cells were seeded in astromal and stromal conditions with a PEGSSDA cross-linker. After 48 h in 3D culture in DMEM or CM, hydrogels were washed three times with sterile PBS and switched to fresh DMEM containing 2% (vol/vol) FBS. After 24 h, spent media samples were collected and compared with fresh media in biological triplicate using the YSI analyzer. PEGSSDA-based hydrogels were dissociated using 40 mM N-acetyl-cysteine (NAC) for 60–120 min per the manufacturer's protocol, and cells were counted. Metabolite consumption was calculated by subtracting spent media measurements from fresh media measurements and normalizing to cell number.

Metabolomics. For steady-state intracellular metabolite profiling, PDAC cells were seeded in 3D cultures (5 × 10⁵ cells per mL hydrogel, 1 mL hydrogel per well in six-well plates) on day 1, and changed to DMEM containing 2% (vol/vol) FBS (astromal) or CM containing 2% (vol/vol) FBS (stromal) on day 2. On day 3, cell media was replaced with fresh media 2 h before extraction. Media was aspirated, and cold (–80 °C) methanol was added to each well while plates were on dry ice. After 30 min of incubation at –80 °C, hydrogels and methanol were scraped and transferred to prechilled tubes, and samples were centrifuged at 3,000 × g for 10 min at 4 °C. Supernatants were recovered, centrifugation repeated, and supernatants dried down in a refrigerated speedvac and stored at –80 °C until analysis. Cells seeded in parallel were analyzed by CellTiter-Glo, and results were used for normalization. Metabolites were analyzed in biological triplicate by liquid chromatography–MS/MS using selected reaction monitoring (SRM) in a 5500 QTRAP hybrid triple quadrupole mass spectrometer (AB/SCIEX) coupled to a Prominence UFLC HPLC system (Shimadzu). Data analysis was performed in MetaboAnalyst 3.0.

Western Blot Analysis. Western blots were performed as previously described (15). Antibody information and additional details can be found in [SI Materials and Methods](#).

Chromatin Immunoprecipitation and ChIP-Seq. For ChIP and ChIP-Seq experiments under astromal and stromal conditions, 3D cultures were constructed using the PEGSSDA cross-linker to facilitate rapid dissociation. ChIP, deep sequencing, and analysis were performed as described previously (35). For additional details, see *SI Materials and Methods*.

Orthotopic Transplant Studies. The p53 2.1.1 luciferase-expressing PDAC cell line was used for orthotopic transplantation into immune-competent FVB/n hosts, as previously described (45). All mouse experiments were performed with the approval of the institutional animal care and use committee (IACUC) of the Salk Institute. For further details, see *SI Materials and Methods*.

ACKNOWLEDGMENTS. We thank P. Phojanakong, D. Wang, J. Alvarez, and H. Juguilon for technical assistance; J. Bradner for providing JQ1; and H. Stoppler

and the UCSF Helen Diller Family Comprehensive Cancer Center Tissue Core for providing fresh-frozen human PDAC samples. This work was funded by NIH Grants DK057978, HL105278, DK090962, HL088093, ES010337, and CA014195 (to R.M.E.), K99CA188259 (to M.H.S.), and R01GM095567 (to A.C.K.); National Cancer Institute Grants R01CA15749, R01CA188048, and P01CA117969; ACS Research Scholar Grant RSG-13-298-01-TBG; the Glenn Foundation for Medical Research; Leona M. and Harry B. Helmsley Charitable Trust Grant 2012-PG-MED002; and Ipsen/Biomeasure. R.M.E. and M.D. were supported in part by a Stand Up to Cancer Dream Team Translational Cancer Research Grant, a Program of the Entertainment Industry Foundation (SU2C-AAAC-DT0509). R.M.E. is an investigator of the Howard Hughes Medical Institute and March of Dimes Chair in Molecular and Developmental Biology at the Salk Institute and is supported by a grant from the Lustgarten Foundation and a gift from the Freeberg Foundation.

- Potter JD (2007) Morphogens, morphostats, microarchitecture and malignancy. *Nat Rev Cancer* 7(6):464–474.
- Bissell MJ, Hines WC (2011) Why don't we get more cancer? A proposed role of the microenvironment in restraining cancer progression. *Nat Med* 17(3):320–329.
- Apte M, Pirola RC, Wilson JS (2015) Pancreatic stellate cell: Physiologic role, role in fibrosis and cancer. *Curr Opin Gastroenterol* 31(5):416–423.
- Hanahan D, Coussens LM (2012) Accessories to the crime: Functions of cells recruited to the tumor microenvironment. *Cancer Cell* 21(3):309–322.
- Ying H, et al. (2016) Genetics and biology of pancreatic ductal adenocarcinoma. *Genes Dev* 30(4):355–385.
- Riss J, et al. (2006) Cancers as wounds that do not heal: Differences and similarities between renal regeneration/repair and renal cell carcinoma. *Cancer Res* 66(14):7216–7224.
- Quail DF, Joyce JA (2013) Microenvironmental regulation of tumor progression and metastasis. *Nat Med* 19(11):1423–1437.
- Guerra C, et al. (2007) Chronic pancreatitis is essential for induction of pancreatic ductal adenocarcinoma by K-Ras oncogenes in adult mice. *Cancer Cell* 11(3):291–302.
- Provenzano PP, et al. (2012) Enzymatic targeting of the stroma ablates physical barriers to treatment of pancreatic ductal adenocarcinoma. *Cancer Cell* 21(3):418–429.
- Jacobetz MA, et al. (2013) Hyaluronan impairs vascular function and drug delivery in a mouse model of pancreatic cancer. *Gut* 62(1):112–120.
- Feig C, et al. (2013) Targeting CXCL12 from FAP-expressing carcinoma-associated fibroblasts synergizes with anti-PD-L1 immunotherapy in pancreatic cancer. *Proc Natl Acad Sci USA* 110(50):20212–20217.
- Beatty GL, et al. (2015) Exclusion of T cells from pancreatic carcinomas in mice is regulated by Ly6C F4/80 extra-tumor macrophages. *Gastroenterology* 149(1):201–210.
- Riopel MM, Li J, Liu S, Leask A, Wang R (2013) β 1 integrin-extracellular matrix interactions are essential for maintaining exocrine pancreas architecture and function. *Lab Invest* 93(1):31–40.
- Willson JS, Pirola RC, Apte MV (2014) Stars and stripes in pancreatic cancer: Role of stellate cells and stroma in cancer progression. *Front Physiol* 5:52.
- Sherman MH, et al. (2014) Vitamin D receptor-mediated stromal reprogramming suppresses pancreatitis and enhances pancreatic cancer therapy. *Cell* 159(1):80–93.
- Waghay M, et al. (2016) GM-CSF mediates mesenchymal-epithelial cross-talk in pancreatic cancer. *Cancer Discov* 6(8):886–899.
- Sousa CM, et al. (2016) Pancreatic stellate cells support tumour metabolism through autophagic alanine secretion. *Nature* 536(7617):479–483.
- Rhim AD, et al. (2014) Stromal elements act to restrain, rather than support, pancreatic ductal adenocarcinoma. *Cancer Cell* 25(6):735–747.
- Özdemir BC, et al. (2014) Depletion of carcinoma-associated fibroblasts and fibrosis induces immunosuppression and accelerates pancreas cancer with reduced survival. *Cancer Cell* 25(6):719–734.
- Lee JJ, et al. (2014) Stromal response to Hedgehog signaling restrains pancreatic cancer progression. *Proc Natl Acad Sci USA* 111(30):E3091–E3100.
- Boj SF, et al. (2015) Organoid models of human and mouse ductal pancreatic cancer. *Cell* 160(1–2):324–338.
- Ying H, et al. (2012) Oncogenic Kras maintains pancreatic tumors through regulation of anabolic glucose metabolism. *Cell* 149(3):656–670.
- Bayne LJ, et al. (2012) Tumor-derived granulocyte-macrophage colony-stimulating factor regulates myeloid inflammation and T cell immunity in pancreatic cancer. *Cancer Cell* 21(6):822–835.
- Pylayeva-Gupta Y, Lee KE, Hajdu CH, Miller G, Bar-Sagi D (2012) Oncogenic Kras-induced GM-CSF production promotes the development of pancreatic neoplasia. *Cancer Cell* 21(6):836–847.
- Kamphorst JJ, et al. (2015) Human pancreatic cancer tumors are nutrient poor and tumor cells actively scavenge extracellular protein. *Cancer Res* 75(3):544–553.
- Dangi-Garimella S, Sahai V, Ebine K, Kumar K, Munshi HG (2013) Three-dimensional collagen I promotes gemcitabine resistance in vitro in pancreatic cancer cells through HMG2-dependent histone acetyltransferase expression. *PLoS One* 8(5):e64566.
- Lee JV, et al. (2014) Akt-dependent metabolic reprogramming regulates tumor cell histone acetylation. *Cell Metab* 20(2):306–319.
- Delmore JE, et al. (2011) BET bromodomain inhibition as a therapeutic strategy to target c-Myc. *Cell* 146(6):904–917.
- Winston F, Allis CD (1999) The bromodomain: A chromatin-targeting module? *Nat Struct Biol* 6(7):601–604.
- Dhalluin C, et al. (1999) Structure and ligand of a histone acetyltransferase bromodomain. *Nature* 399(6735):491–496.
- Dawson MA, et al. (2011) Inhibition of BET recruitment to chromatin as an effective treatment for MLL-fusion leukaemia. *Nature* 478(7370):529–533.
- Mazur PK, et al. (2015) Combined inhibition of BET family proteins and histone deacetylases as a potential epigenetics-based therapy for pancreatic ductal adenocarcinoma. *Nat Med* 21(10):1163–1171.
- Zeng L, Zhou MM (2002) Bromodomain: An acetyl-lysine binding domain. *FEBS Lett* 513(1):124–128.
- Florence B, Fallier DV (2001) You bet-cha: A novel family of transcriptional regulators. *Front Biosci* 6:D1008–D1018.
- Ding N, et al. (2013) A vitamin D receptor/SMAD genomic circuit gates hepatic fibrotic response. *Cell* 153(3):601–613.
- Roy N, et al. (2015) Brg1 promotes both tumor-suppressive and oncogenic activities at distinct stages of pancreatic cancer formation. *Genes Dev* 29(6):658–671.
- Gosselin D, et al. (2014) Environment drives selection and function of enhancers controlling tissue-specific macrophage identities. *Cell* 159(6):1327–1340.
- Lavin Y, et al. (2014) Tissue-resident macrophage enhancer landscapes are shaped by the local microenvironment. *Cell* 159(6):1312–1326.
- Yosimichi G, et al. (2001) CTGF/Hcs24 induces chondrocyte differentiation through a p38 mitogen-activated protein kinase (p38MAPK), and proliferation through a p44/42 MAPK/extracellular-signal regulated kinase (ERK). *Eur J Biochem* 268(23):6058–6065.
- Day RM, Cioce V, Breckenridge D, Castagnino P, Bottaro DP (1999) Differential signaling by alternative HGF isoforms through c-Met: Activation of both MAP kinase and PI 3-kinase pathways is insufficient for mitogenesis. *Oncogene* 18(22):3399–3406.
- Baxter RC (2014) IGF binding proteins in cancer: Mechanistic and clinical insights. *Nat Rev Cancer* 14(5):329–341.
- Kiuchi N, et al. (1999) STAT3 is required for the gp130-mediated full activation of the c-myc gene. *J Exp Med* 189(1):63–73.
- Hirano T, Ishihara K, Hibi M (2000) Roles of STAT3 in mediating the cell growth, differentiation and survival signals relayed through the IL-6 family of cytokine receptors. *Oncogene* 19(21):2548–2556.
- Nowak DG, et al. (2015) MYC drives Pten/Trp53-deficient proliferation and metastasis due to IL6 secretion and AKT suppression via PHLPP2. *Cancer Discov* 5(6):636–651.
- Collisson EA, et al. (2012) A central role for RAF→MEK→ERK signaling in the genesis of pancreatic ductal adenocarcinoma. *Cancer Discov* 2(8):685–693.
- Dobin A, et al. (2013) STAR: Ultrafast universal RNA-seq aligner. *Bioinformatics* 29(1):15–21.
- Trapnell C, et al. (2013) Differential analysis of gene regulation at transcript resolution with RNA-seq. *Nat Biotechnol* 31(1):46–53.
- Roberts A, Trapnell C, Donaghey J, Rinn JL, Pachter L (2011) Improving RNA-Seq expression estimates by correcting for fragment bias. *Genome Biol* 12(3):R22.
- Saldanha AJ (2004) Java Treeview—Extensible visualization of microarray data. *Bioinformatics* 20(17):3246–3248.
- Wang J, Duncan D, Shi Z, Zhang B (2013) WEB-based Gene Set Analysis Toolkit (WebGestalt): Update 2013. *Nucleic Acids Res* 41(Web Server issue):W77–W83.
- Zhang B, Kirov S, Snoddy J (2005) WebGestalt: An integrated system for exploring gene sets in various biological contexts. *Nucleic Acids Res* 33(Web Server issue):W741–W748.
- Hsiao A, Worrall DS, Olefsky JM, Subramaniam S (2004) Variance-modeled posterior inference of microarray data: Detecting gene-expression changes in 3T3-L1 adipocytes. *Bioinformatics* 20(17):3108–3127.
- Subramaniam A, et al. (2005) Gene set enrichment analysis: A knowledge-based approach for interpreting genome-wide expression profiles. *Proc Natl Acad Sci USA* 102(43):15545–15550.
- Mootha VK, et al. (2003) PGC-1 α -responsive genes involved in oxidative phosphorylation are coordinately downregulated in human diabetes. *Nat Genet* 34(3):267–273.
- Barish GD, et al. (2010) Bcl-6 and NF- κ B cistromes mediate opposing regulation of the innate immune response. *Genes Dev* 24(24):2760–2765.
- Heinz S, et al. (2010) Simple combinations of lineage-determining transcription factors prime cis-regulatory elements required for macrophage and B cell identities. *Mol Cell* 38(4):576–589.